ASEN 2002 - Lab 3

Katelyn Griego, * Jordan Lerner, † Nicholas Renninger, ‡ Alexis Sotomayor §

University of Colorado - Boulder

This lab's objective was primarily to learn how a wind tunnel operates and how different devices' measurements of differential pressures allows for the calculation of the velocities of airflow within the wind tunnel. Bernoullis principle, valid here as the wind tunnel operates at low enough speeds such that the flow can be considered incompressible, can be then utilized to analyze the air speeds at different points in the flow as function of these differential pressure measurements. Additionally, the calibration of the wind tunnel using a voltage control of the suction fan was investigated, leading to the discovery of a concrete, linear model of the air speed in the test section of the wind tunnel as a funcion of this control voltage. Boundary layers, which are regions of velocity deficit flow, were analyzed and the maximum boundary layer thickness was calculated to be 7.3 millimeters. Subsequently, error analysis was performed on the airspeed data to determine the largest source of error, which was clearly the contribution of the differential pressure transducer. The analysis suggests the uncertainty in the airspeed gradually decreases as the velocity of the flow increases, an encouraging result for high-speed testing in the tunnel.

Nomenclature

δV = Uncertainty in airspeed (m/s)
ρ = Density (kg/m^3)
A_1 = Area of the settling chamber (m)
A_2 = Area of the test-section (m)
P_{atm} = Atmospheric Pressure (Pa)
R = Gas constant for air (kJ/kgK)
T_{atm} = Atmospheric Temperature (K)
V_0 = Velocity in the settling chamber (m/s)
V_∞ = Free stream velocity (m/s)
V_s = Velocity in the test-section (m/s)

*103380164
†105510900
‡105492876
§105225132

I. Introduction

The goal of this lab is to recognize basic concepts and definitions associated with flow measurements and wind tunnel testing. Wind tunnels are utilized to learn about how a flow can physically interact with a "stationary" test body placed in the flow. In the ITLL, there is a Low-Speed Wind Tunnel in which data is collected. The motivation for the experiment is to develop a fundamental understanding of how this wind tunnel operates by calibration of the test section. After the experiment, airspeed is to be computed through a number of equations that relate to different pressure-measuring devices implemented in the wind tunnel. Understanding the limitations of the measurements can be found by a detailed analysis of the uncertainty in the airspeed measurement. It is not acceptable to make the assumption that the velocity throughout the test-section is uniform and constant. For this reason the variation in the airspeed needs to be calculated. The differential pressure is measured with static-ring ports and a pitot-static probe.

Using Bernoulli's equation for incompressible flow, the pressure at various locations can be related to the square of the velocity to determine the airspeed. This equation requires knowledge of the density of the fluid, which can determined by using the the equation of state for a perfect gas, incorporating the gas constant for air along with the ambient temperature and pressure values measured during the experiment. Only one point of temperature and pressure must be measured since density for incompressible flow is assumed to be constant. The density of the fluid can then be solved for to directly relate differential pressure to the airspeed at various locations.

II. Experimental Setup and Measurement Techniques

The ITLL Low-Speed Wind Tunnel is an Eiffel, open-circuit, suction type wind tunnel. Air is pulled through the closed test-section of the wind tunnel by a bladed fan driven by an electric motor. A schematic of the wind tunnel can be seen in Figure 1. Temperature and pressure can be directly measured from the wind-tunnel itself. The ambient temperature measurements are made with an LM35 Precision Centigrade Temperature Sensor from National Semiconductor. Pressure measurements consist of absolute, gauge, and differential pressures. An absolute pressure measurement device computes the magnitude of pressure relative to a vacuum. On the other hand, a gauge pressure measurement device computes the pressure relative to the atmospheric pressure. The relative pressure difference between two locations is computed by the differential pressure measurement device. A U-tube manometer, a differential transducer, and an absolute pressure transducer are used to take these measurements.

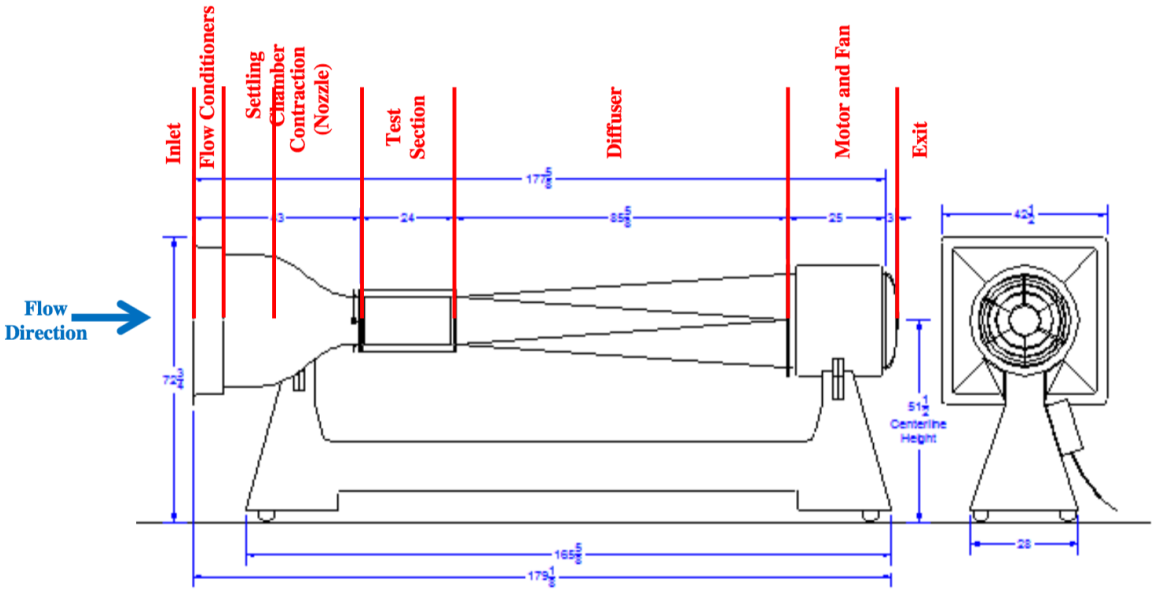

Figure 1. A schematic of the ITLL Low-Speed Wind Tunnel

Before collecting data, the tunnel was inspected and the pressure tubes were located. The next step was to connect the pressure disconnects according to the configuration that was specified for the group. The water manometer was connected to the pitot-static probe and the airspeed pressure transducer was connected to the static rings. The wind tunnel door was then closed and locked. Before collecting data, the airspeed and pressure transducers are zeroed and the first voltage was assigned. Once the wind tunnel reached equilibrium measurements on the U-tube manometer and the pressure transducer, the transducer measurements are taken and saved and the manometer data was manually recorded. This process is repeated for all assigned voltages.

For the second task the wind tunnel is brought back to zero. After a few connections are made, the leading edge of the ELD Boundary Layer probe is aligned downstream of the static port on the base of the test section (port 9 for our group). The probe is moved until the tip is just barely touching the wind tunnel floor. The airspeed and pressure transducers are zeroed once again. The desired voltage is set and the measurements at the assigned locations are taken, moving the ELD pitot probe up in the flow until it reached the center line of the wind tunnel. This allowed for a continuous measurement of the differential pressure as a function of height in the flow, so that the velocity of the flow in the boundary layer could be compared to that of the free-stream velocity.

The data taken was compared with that of group five that was taken on the same day (section 013). Group five's measurements of the pitot-static were taken with a transducer at the same voltages. Therefore, a comparison is able to be made between the transducer and manometer measurements. The rest of the data for all other groups in all other sections was then compiled, sorted and subsequently analyzed as outlined in the following sections.

III. Airspeed Calculation and Airspeed Model

Variations of Bernoulli's Equation were utilized in order to compute the airspeed. Because the wind tunnel is demonstrative of a low speed, subsonic flow, the flow can be assumed to be in-compressible (where Mach number is less than 0.3), making the density constant. When using the pitot-static probe, it is assumed that the velocity of the air is isentropically slowed to zero at the front of the probe, V = 0. The density of the air can be solved by obtaining the ambient pressure and the ambient temperature, in conjunction with the gas constant for air. We are treating air as an ideal gas, and can use the equation of state to relate these values to find the air's local density. The pitot-static probe is mounted in the wind tunnel to allow for calculation of the pressure differential, the difference between the static pressure and the total pressure at that point in the flow. The following derivation of Bernoulli's equation is utilized for the calculation of airspeed:

$$V_\infty = \sqrt{2\Delta P \frac{P_{atm}}{RT_{atm}}} = \sqrt{\frac{2\Delta P}{\varrho}} \tag{1}$$

Another method to evaluate differential pressure, and in turn the airspeed, is to treat the wind tunnel as a large Venturi tube. When using the Venturi tube, this method measures static pressure in both the settling chamber and the test section, using the static rings installed in the ITLL wind tunnel. Bernoulli's equations can be applied again, however the assumption that V_0 goes to zero cannot be made. The device in this setup measures the average static pressures at two different locations in the wind tunnel. These two measurements are typically performed in the settling chamber and in the test section, and then are placed into the following equation, along with the ratio of the test section cross sectional area to the settling chamber cross sectional area. The equation for this scenario is detailed below:

$$V_\infty = \sqrt{\frac{2\Delta P R T_{atm}}{P_{atm}(1 - (\frac{A_2}{A_1})^2)}} \tag{2}$$

III.A. Airspeed Results

The results of the analysis of the all data gathered across all groups is shown in Figure 2, which shows the air velocity measured at all voltages from $0.5 - 10\,Volts$ using the pitot-static probe and the static rings. It also shows the model developed for controlling the air velocity, as a linear function of voltage, which is detailed in Section III.C. Observing Figure 2, it is clear that the two methods of measurement - the pitot-static probe and the static rings - yield extremely, almost indistinguishably similar measurements of air velocity in the

wind tunnel. Also, as discussed in Section IV, the uncertainty in these measurements uniformly decreases as V_∞ increases.

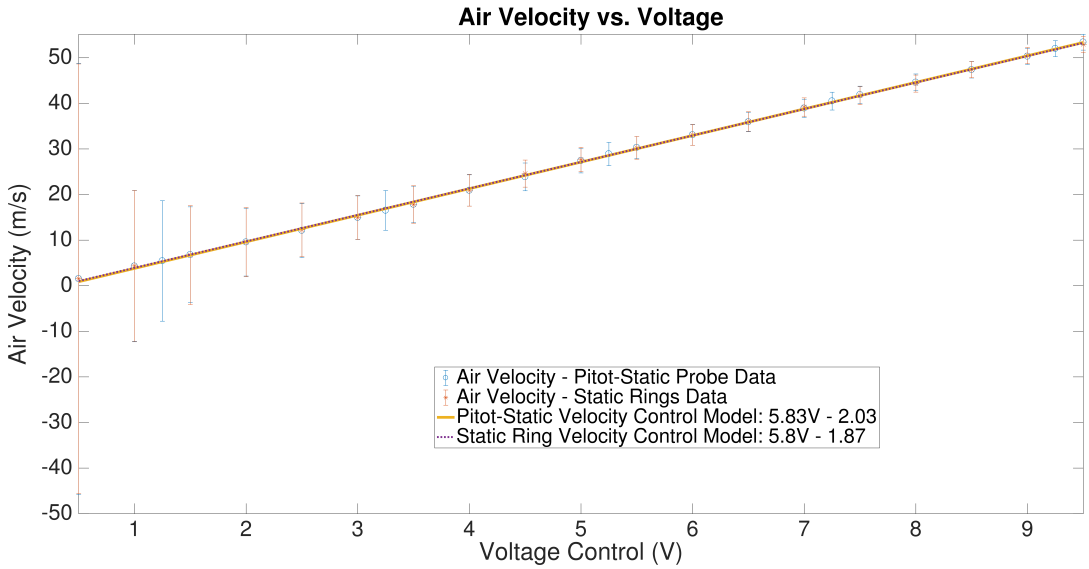

Figure 2. This shows the profile of air velocity as a function of voltage with uncertainty, utilizing every data point taken by every group, in every section. *Measurements taken by both the pitot-static probe and by the static rings are shown. Error bars show uncertainty in the air velocity for averaged data points for each measured voltage. Along with the experimental data, the specific voltage to air velocity mapping model is shown for each measurement device.*

III.B. U-Tube Manometer versus Pressure Transducer

While seemingly unexpected, the manometer appears to produce more precise measurement of the differential pressure in the wind tunnel, as shown in Figure 3. We found $\delta_{manometer,height} = 0.25$ in., which makes the uncertainty in differential pressure $\delta_{manometer,pressure} = 51.438$ Pa, which is actually an overestimate of the uncertainty, based on the difficulty of accurately reading the meniscus of the manometer fluid. The differential pressure transducer was found to have a constant uncertainty of approximately 1% of its full-scale reading, $\delta_{transducer} = 68.98$ Pa.

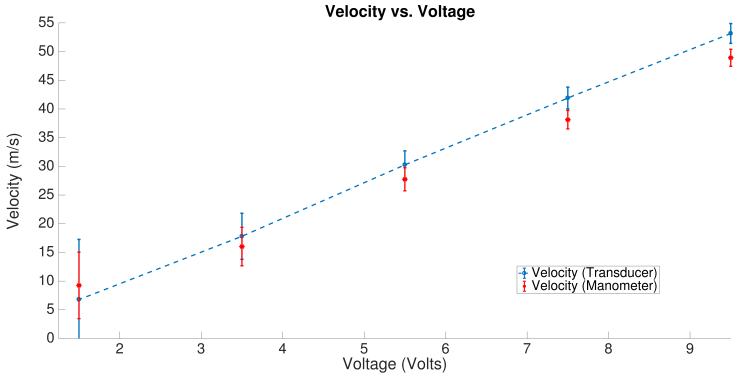

Figure 3. Comparison of Pressure Transducer and the U-tube Manometer for taking differential pressure measurements. of a pitot-static probe. *The manometer can be seen to actually be more precise than the pressure transducer, even with an overestimated uncertainty of* $\delta_{manometer,pressure} = 51.438$ *Pa.*

Therefore, we observed more precise measurements of the differential pressure in the pitot-static probe using the manometer than did Group 5, which used the pressure transducer. However, the manometer probably suffers from inaccuracy in its measurement, as it can be seen to give consistently low values for air velocity as compared to the more accurate pressure transducer.

III.C. Air Velocity Model

The voltage to velocity model we developed was determined based on a linear curve fitting of the experimental data shown in Figure 2. This model was plotted in the same figure, and is nominally:

$$V_\infty = 5.83 \cdot v - 2.03 \quad (pitot - static\, probe) \tag{3}$$

$$V_\infty = 5.80 \cdot v - 1.87 \quad (static\, rings) \tag{4}$$

Here, v is defined from $0.5 \leq v \leq 10$ volts. v is chosen to remain above 0.5 volts, as below 0.5 volts, the airspeed measurements are so imprecise that any airspeed measurement taken at such low speeds results in a meaningless airspeed measurement.

IV. Airspeed Measurement Uncertainty

To calculate the uncertainty in airspeed, we must use the general formula given below in Equation 5. The general formula will be used four times to quantify the uncertainty in the velocity for both measurement devices, the differential pressure transducer and the U-tube manometer. Partial derivatives are taken from the velocity equation with respect to the independent variables i.e. the change in pressure, the atmospheric pressure, and the atmospheric temperature. The individual errors associated with the independent variables are incorporated in the general formula. These errors are given in the lab document by the manufacturer or described in Section III.B. above for the manometer.

$$\delta V = \sqrt{(\frac{\partial V}{\partial \Delta P}\delta \Delta P)^2 + (\frac{\partial V}{\partial P_{atm}}\delta P_{atm})^2 + (\frac{\partial V}{\partial T_{atm}}\delta T_{atm})^2} \tag{5}$$

IV.A. Airspeed Uncertainty versus Airspeed

The uncertainty for the differential pressure transducer and the uncertainty for the U-tube manometer are very similar. The uncertainties were calculated at each data point. When plotted in Figures 4 & 5, it can be observed that both uncertainties follow the same pattern. The uncertainty in the airspeed starts off very large, and as the airspeed increases, the uncertainty in the measurement of air velocity becomes smaller and smaller. The error bars plotted in Figures 2 & 3 also demonstrate decreasing uncertainty in the velocity measurement as the velocity increases.

As the quoted accuracy of the differential pressure is based on the full scale range - i.e. it is fixed to a certain value proportional to the maximum value that can be read by the instrument - the uncertainty when measuring small values of pressure is substantially worse than when measuring larger pressure values. Essentially, when the measurements are small enough, their magnitudes become almost the same as the magnitudes of the uncertainties in the measurements. Thus, the overall uncertainty contribution of the device to the uncertainty in the calculation of velocity becomes very large as the pressure becomes small.

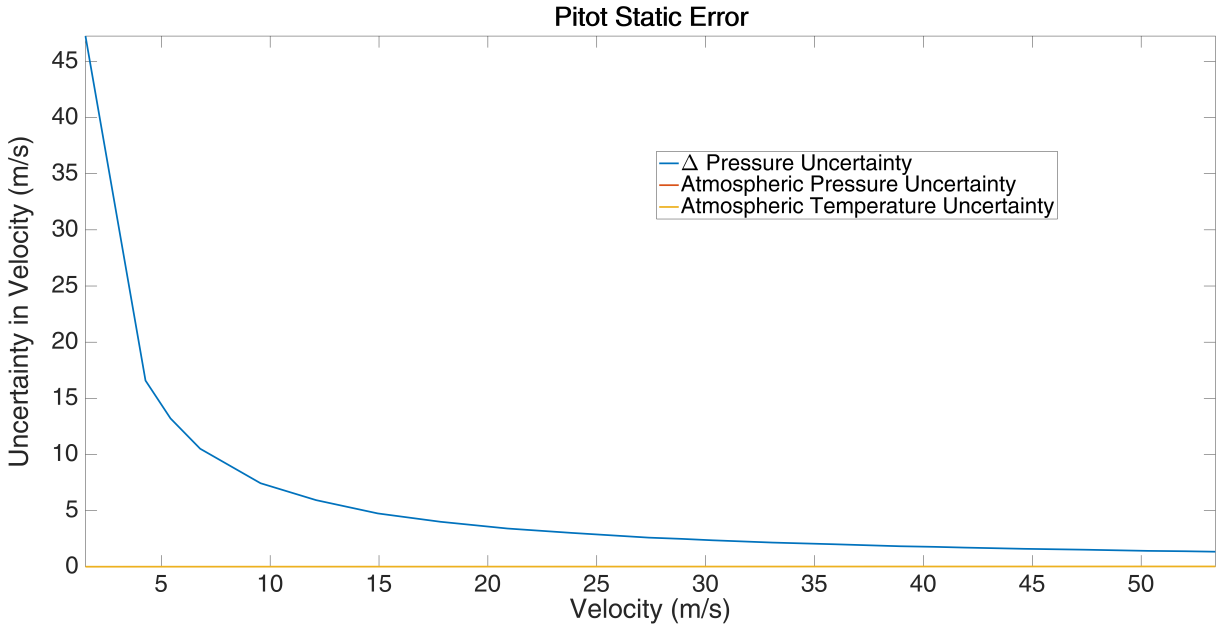

Figure 4. This plot shows the contributions of each of the three independent sources of error to the overall uncertainty in the measurement of air velocity in the wind tunnel by the pitot-static probe. *The differential pressure gauge can be seen to be contributing the majority of the overall uncertainty to the air velocity uncertainty.*

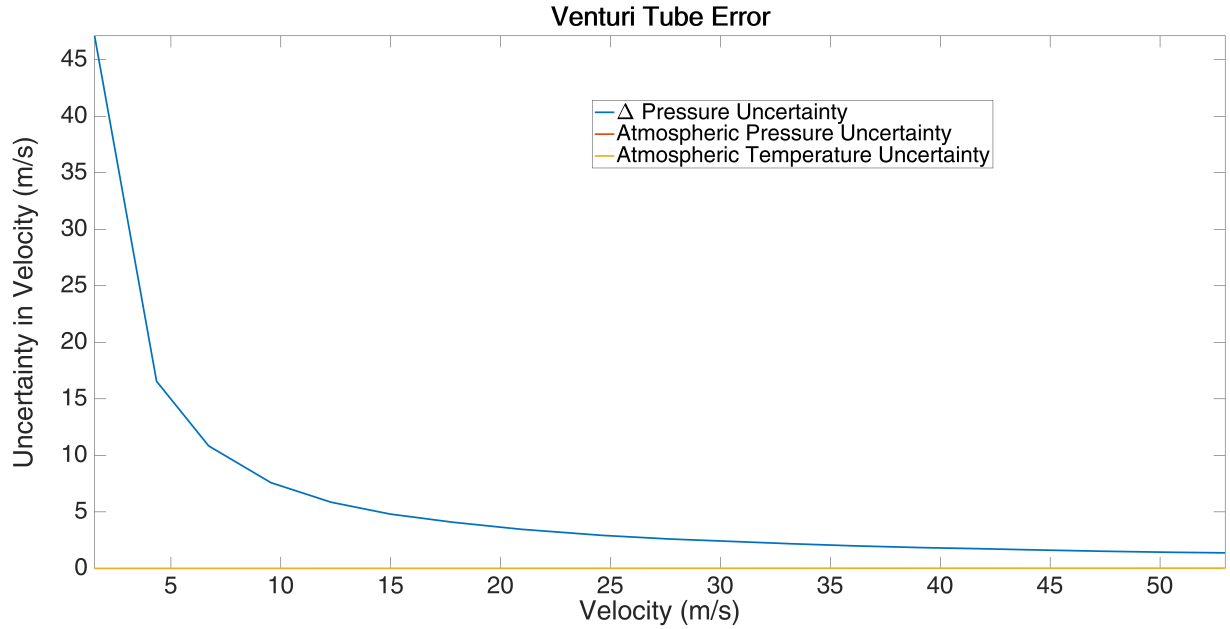

Figure 5. This plot shows the contributions of each of the three independent sources of error to the overall uncertainty in the measurement of air velocity in the wind tunnel by the static rings. *The differential pressure gauge can be seen to be contributing the majority of the overall uncertainty to the air velocity uncertainty.*

IV.B. Sources of Uncertainty

The largest source of uncertainty is caused by the measurements of the differential pressure made by the differential pressure transducer. This effect can also be observed by the visualization of Eqn. 5 in Figures 4 & 5. The most obvious way that the system precision can be improved is to use a differential pressure gauge with a lower manufacturer uncertainty, perhaps one that has an error in measurement based on its current reading and not on its full-scale reading. This way, the uncertainty in the measurement of velocity would be more consistent, and it would make testing at lower air speeds more accurate. When using a U-tube manometer, an increase in the number of measurements taken would allow for more data to analyze height differences between levels.

IV.C. Accuracy of U-Tube Manometer

The U-tube manometer provides a surprisingly more accurate measurement of the velocity than the pressure transducer. The height of the fluid in the manometer has gradations every tenth of an inch, and we allowed for approximately $0.25in.$ of variability because of the difficulty in properly reading the meniscus. As a result, the manometer is not incredibly accurate, but still allows for very reliable measurement of airspeed if read properly. The pressure transducer, on the other hand, records the differential pressure electronically 20 times per second with an accuracy of 1% of its full-scale range. It therefore has a constant uncertainty for all pressure measurements, which leads to the phenomena of decreased uncertainty in velocity as the pressure - and thus velocity - measurements increase.

V. Boundary Layer Influence

The boundary layer is the result of viscous effects in a flow moving along a body in the air stream. In order to calculate the thickness of the boundary layer, the velocity of the flow was computed by measuring the pressure difference between an ELD pitot probe and a static port along the bottom of the test section. The ELD probe was moved upwards from the base of the test section until it reached the center line of the test section, all while recording the differential pressure at every height in the flow. We then could find the velocity of the flow at every height measured. By finding the velocity of the flow as a continuous function of the height in the flow, we could then compute the height of the boundary layer. We found this height by utilizing the 95% rule, where the height of the boundary layer is defined as where the flow velocity in the boundary layer reaches 95% of the free stream velocity: $V_{boundary\,layer} = 0.95 \cdot V_\infty$.

V.A. Boundary Layer Comparisons

The experimental data obtained on the height of the boundary layer, as visualized in Figure 6, demonstrates how the boundary layer increases non-linearly with increasing distance from the beginning of the test section. Our group's boundary layer height of $6.5\,mm$ at port 9 - located at $0.429\,m$ - is less than that of the groups that measured the boundary layer to be $7.3\,mm$ high at port 11 - located at $0.479\,m$. This is the expected trend for this data, and matches reasonably well with the visualization of the turbulent boundary layer as shown in Figure 6.

V.B. Theoretical Boundary Layer versus Expected Boundary Layer

Using the in compressible version of the continuity equation, we were able to predict the expected boundary layer thickness. We did this by finding V_∞ at the exit and beginning of the test section, and then calculating the area the exit flow must be occupying to have the same volumetric flow rate as at the flow at the entrance of the test section. The expected boundary layer thickness is $0.0014m$ or $1.4mm$. This did not match the experimental results, as the experimentally measured boundary layer thickness was measured to be $7.19mm$, which is 5 times greater than the theoretical boundary layer thickness.

This is due to the our fundamental assumption in using the continuity equation: that the velocity inside of the boundary layer is 0 in the cross-sectional area defined by the boundary layer thickness. This is not realistic, as the velocity in the boundary layer is not 0 all the way up to the maximum height of the boundary layer. In fact, the only place in the boundary layer where the velocity of the flow would be 0 should be at the surface of the test section wall, where we enforce the no-slip condition. This assumption of no mass flux through the boundary layer means that we do not account for any of the flow through the boundary layer,

and thus, in order to "make-up" for this lack of mass flux, the theoretical cross-sectional area at the exit of the test section must be much larger than it realistically should be, which in turn decreases the theoretical boundary layer thickness

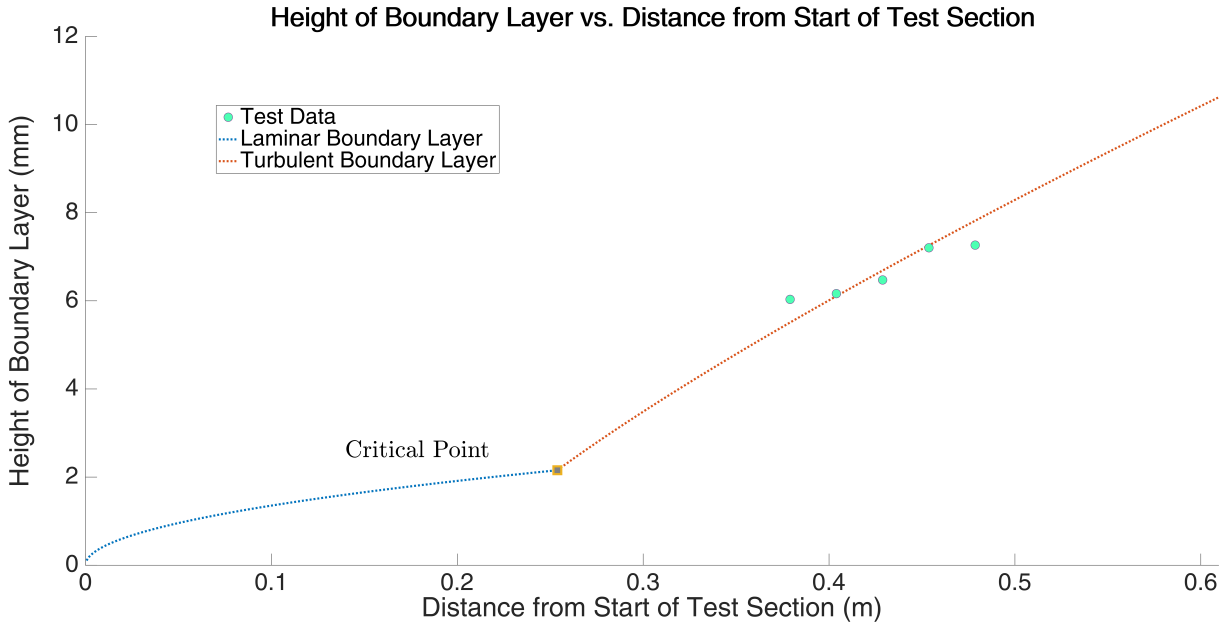

Figure 6. This plot shows the theoretical profile of the boundary layer, the best estimate for the location of the critical point (transition from laminar to turbulent boundary layer), and the experimental data on the measured height of the boundary layer. *The profiles for the laminar and turbulent boundary layer thicknesses are derived from Eqns. 4-91 & 4-99 from the Anderson text. By fitting the line of the turbulent boundary layer to the experimental data, the critical point can be estimated by adjusting* $Re_{x,cr}$.

V.C. Laminar/Turbulent Boundary Layer

From Figure 6, the boundary layer height can be clearly seen to be much too large to be laminar. However, it does not clearly match the turbulent boundary layer profile. Therefore, at ports 7 - 11, the flow is likely at the end of its transition to a turbulent boundary layer and is decidedly not in the laminar regime anymore.

V.D. Theoretical Center line Velocity versus Measured Center line Velocity

The measured increase in the center line velocity came out to be only $0.257\,m/s$ for the experimental data, which came from port 10s differential pressure data, located at the end of the test section. Using the continuity equation and knowledge of boundary layer thickness, the expected center line velocity at the end of the test section was calculated to be $29.94\,m/s$, corresponding with an expected flow increase of $2.77\,m/s$ over the experimental results; an ten fold increase over the actual, measured increase in center line velocity.

These two velocities differ so greatly because the expected results' calculation assumed there was no mass or velocity flux through the boundary layer, which is obviously not the case here, due to the significant mass flux in the boundary layer measured by the non-zero velocity in the experiment. The reasoning behind the larger velocity is based on the same reasoning as in Section V.B, where the assumption of no mass flux in the boundary layer necessitates that the mass flux be increased artificially somewhere else in the theoretical calculation. In this case, this lack of consideration of mass flux through the boundary layer, with a fixed cross-sectional area at the exit of the test section, leads to an increased V_∞ in the theoretical prediction.

VI. Conclusion

Through careful analysis of all of the data taken by the groups, we can conclude several things about the nature of the ITLL Low Speed Wind Tunnel.

First, we have determined that the uncertainty in the velocity in the test section is dependent on the velocity itself, and gets much smaller as the velocity increases. This means that ultra-low velocity testing, with speeds less than $15\,m/s$, is not recommended due to the large uncertainty in the measurement of air speed at these velocities. This means that if we were to change any sensor we had, we would be most benefited by the purchase of a more precise differential pressure gauge, especially one with error based on the measured value and not on the full-scale range. This would reduce the velocity-dependence of the uncertainty in the measurement of air speed.

It would seem that of the four measurement configurations, the static rings connected to the differential pressure transducer would be the best system to use for calculation of the airspeed in the test section. While not as accurate as the manometer, the need for high-speed, high-accuracy data acquisition obviously puts the tedious calculation of airspeed using the manometer out of contention. As compared to the pitot-static probe, with the static rings calibrated properly as they were for this lab, the static rings provide almost identically accurate and precise pressure measurements. The upside of the static rings is that they do not effect the flow in the test section to anywhere near the same degree as the pitot-static probe, and thus the static rings would be better suited to precise measurements in the test section.

The boundary layers did have an appreciable, if not relatively small effect on the center line air speed acceleration. While we could detect a slight acceleration of the flow, the boundary layer still allows for a large mass flux through it, so this acceleration overall does not have an enormous impact on the flow velocity through the test section. However, it still might have an effect on the flow quality, as the boundary layer definitely transitions from laminar to turbulent as it moves through the test section. Therefore, if one was interested in measuring an aerodynamic body in the wind tunnel, it would be advisable to keep it near the center line of the tunnel and to make sure it was as close the to beginning of the test section as possible unless one was interested in studying the laminar-to-turbulent transition or the turbulent boundary layer itself.